Supplementary Material

Secondary organic aerosol origin in an urban environment: influence of biogenic and fuel combustion precursors

M.C. Minguillón[a], N. Pérez[a], N. Marchand[b], A. Bertrand[b], B. Temime-Roussel[b], K. Agrios[c], S. Szidat[c], B. van Drooge[a], A. Sylvestre[b], A. Alastuey[a], C. Reche[a], A. Ripoll[a], E. Marco[a], J. O. Grimalt[a], and X. Querol[a]

[a] Institute of Environmental Assessment and Water Research (IDAEA), CSIC, Barcelona, Spain.

[b] Aix Marseille Université, CNRS, LCE FRE 3416, 13331 Marseille, France.

[c] Department of Chemistry and Biochemistry & Oeschger Centre for Climate Change Research, University of Bern, 3012 Bern, Switzerland.

DOI: 10.1039/c5fd00182j

SECTION S1. General information

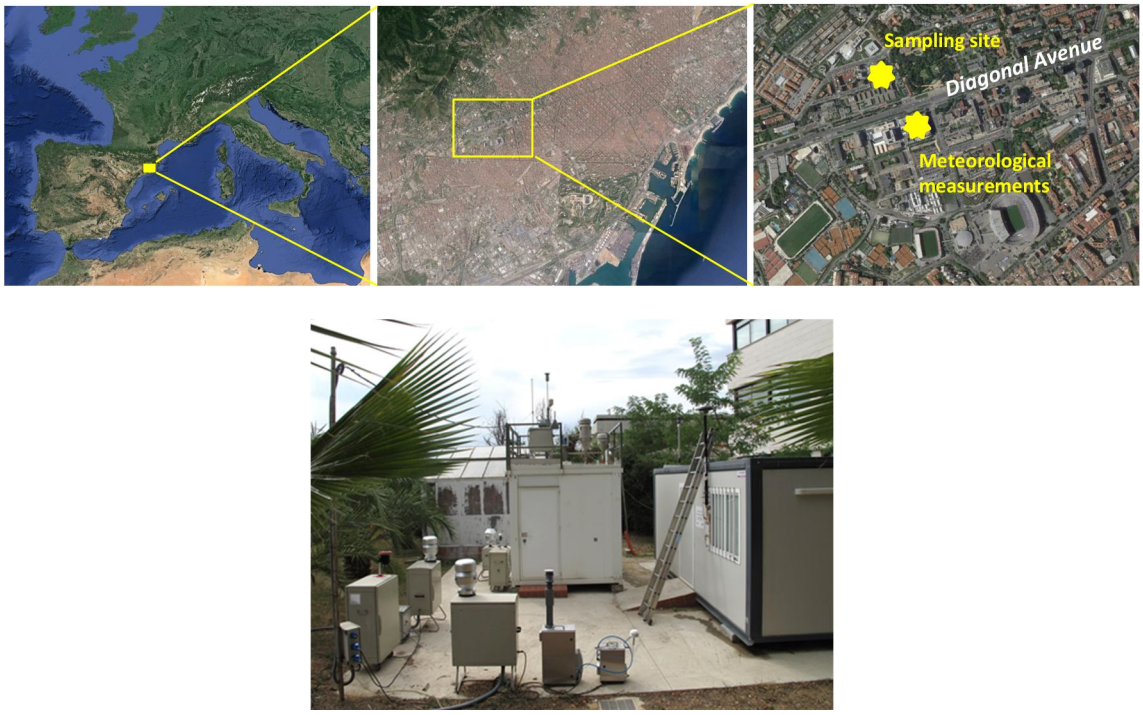

Figure S1. Location of the Palau Reial urban background sampling site in Barcelona and the meteorological measurements point, and general picture of the sampling site.

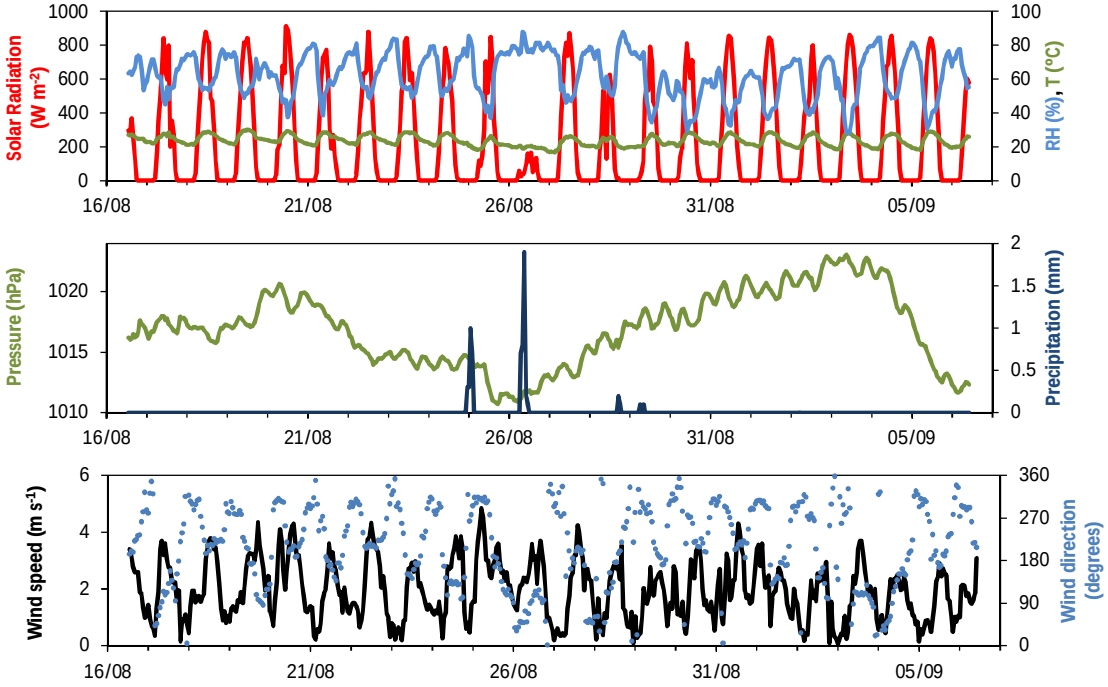

Figure S2. Variation of meteorological parameters during the measurement campaign. Date format is dd/mm.

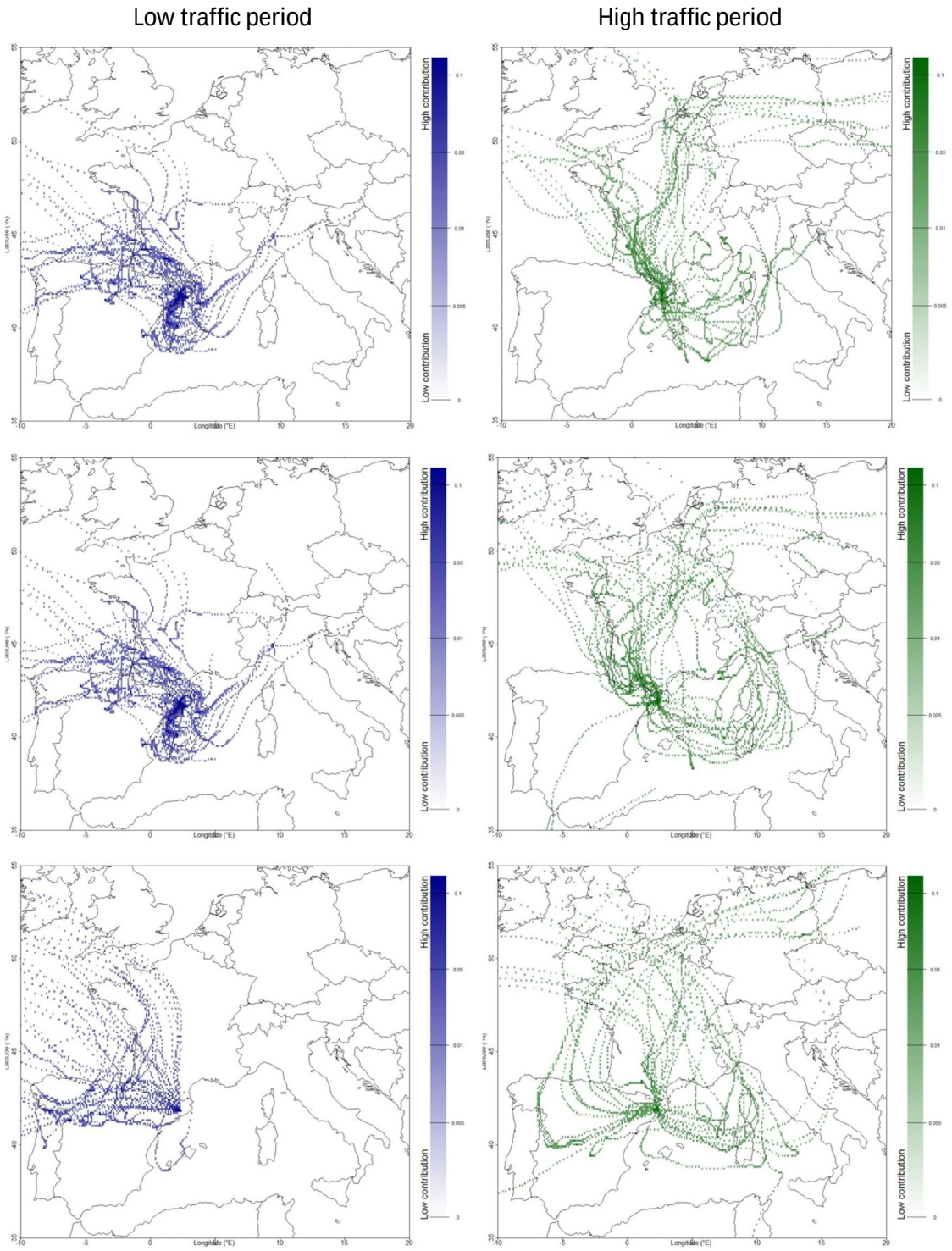

Figure S3. Air mass 5-days back-trajectory densities for the low traffic and the high traffic periods calculated with the HYSPLIT model (Draxler and Rolph, 2015) every 6 hours (0, 6, 12 y 18h) for 750, 1500 and 2500m AGL (top, middle and bottom figures).

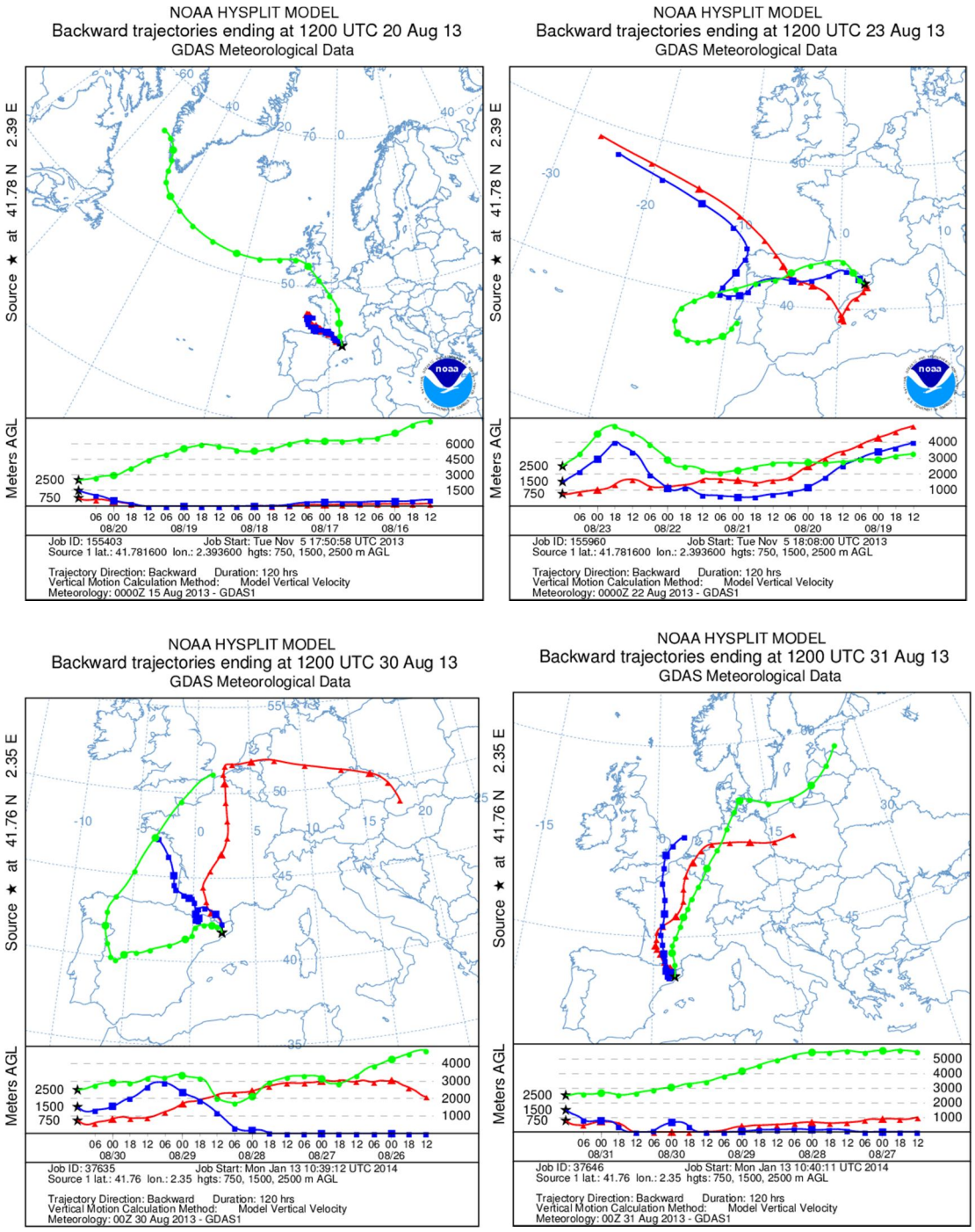

Figure S4. Air mass 5-days back-trajectories for 750, 1500 and 2500m AGL for 20, 23, 30 and 31 August 2013.

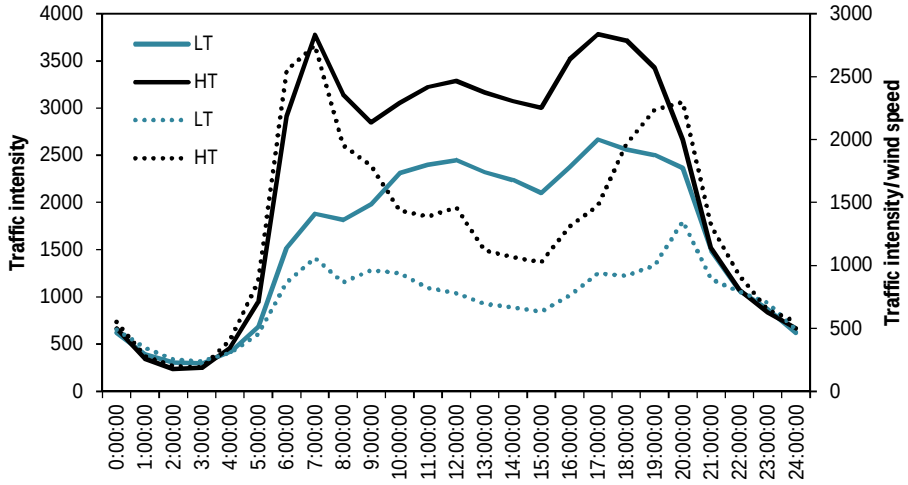

Figure S5. Average intra-day variation of traffic intensity and traffic intensity/wind speed (dotted lines) during low traffic (LT) and high traffic (HT) periods.

SECTION S2. VOCs

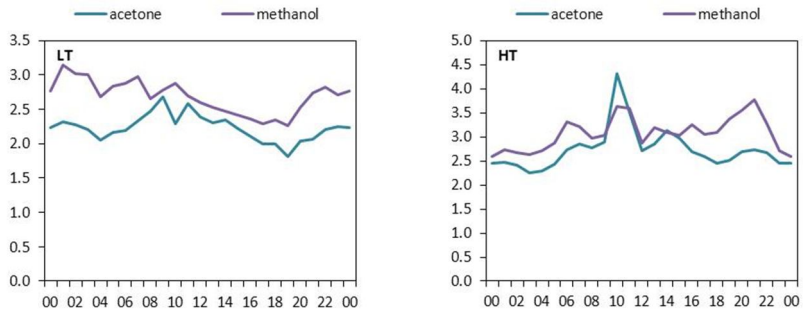

Figure S6. Average daily cycle of the mixing ratios (ppbv) of methanol and acetone during the LT and HT periods. The time is UTC.

SECTION S3. OA source apportionment

Various solutions for the OA source apportionment were explored. A summary of the results are shown below:

2 factors solution. It included a HOA and an OOA factor.

3 factors solution. It included a HOA, a LV-OOA factor and a SV-OOA. The residuals for the m/z 55 showed a daily pattern:

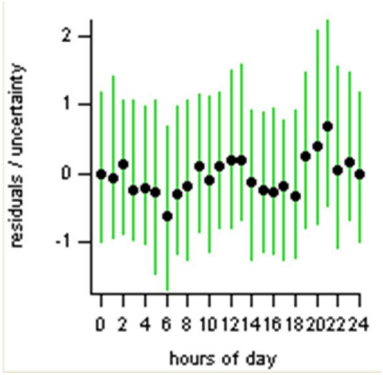

Figure S7. Residuals for m/z 55 for the 3 factors solution.

4 factors solution. It included a HOA, a LV-OOA factor and two SV-OOA factors. The two SV-OOA factors showed a similar diurnal pattern, and their contributions were correlated (R^2=0.5). The f82 for the second SV-OOA factor was 0.007, which is relatively low compared to the IEPOX-OA reference profile (Budisulistiorini et al., 2013), so this profile cannot be interpreted as IEPOX-OA.

5 factors solution. It resulted in a split of the HOA, with the two HOA factors tracking each other (R^2=0.57). The two SV-OOA factors showed a similar diurnal pattern.

4 factors with constrained COA. It included a HOA, a LV-OOA, a SV-OOA and a COA factor. The COA factor was constrained using the COA profile from Mohr et al. (2012). Different a-values from 0.025 to 0.2 in steps of 0.025 were tested. The correlation coefficients of the OA factors contributions with BC concentrations, the correlation coefficient of the HOA profile with the HOA profile from DAURE (Mohr et al., 2012), and the OA factors diurnal patterns are shown below.

a-value for COA	R^2 HOA vs BC	R^2 COA vs BC	R^2 HOA vs COA	R^2 HOA vs HOA_DAURE	Comments	Diurnal patterns
0.025	0.416	<0.1 (one outlier)	0.112	0.9349		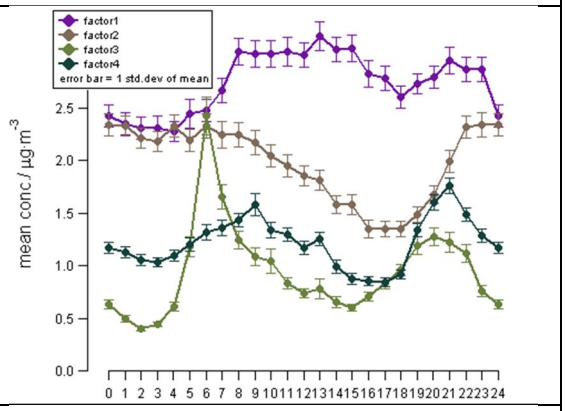
0.05	0.416	0.144	0.146	0.9032	LV has almost only 44, SV almost only 43 (no 44); hence contribution from LV higher than other solutions	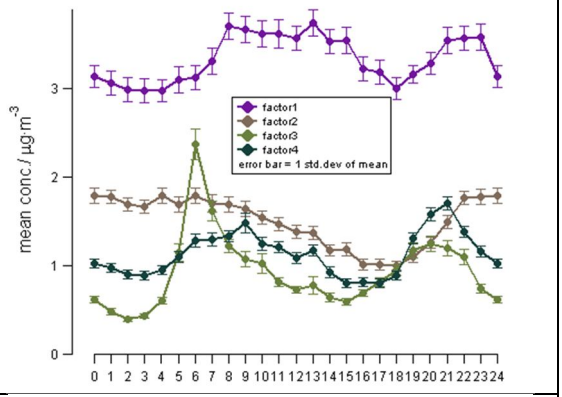
0.075	0.445	0.146	0.151	0.9096	LV has almost only 44, SV almost only 43 (no 44)	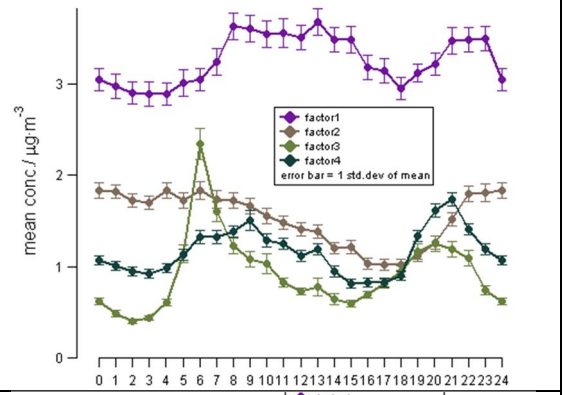
0.1	0.441	0.147	0.141	0.9616		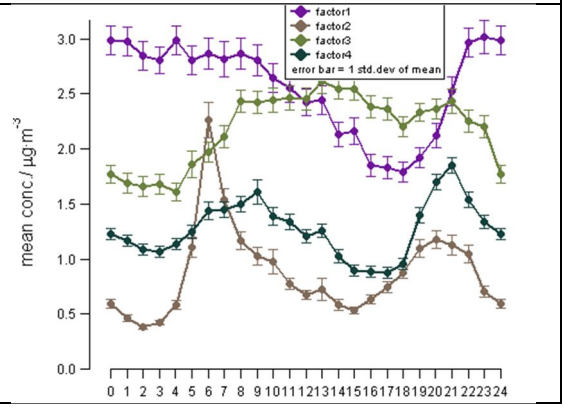

a-value for COA	R^2 HOA vs BC	R^2 COA vs BC	R^2 HOA vs COA	R^2 HOA vs HOA_DAURE	Comments	Diurnal patterns
0.125	0.44	0.147	0.134	0.9581		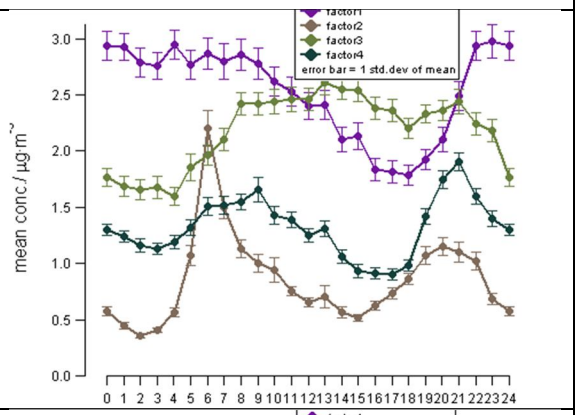
0.15	0.403	0.1301	0.153	0.9503		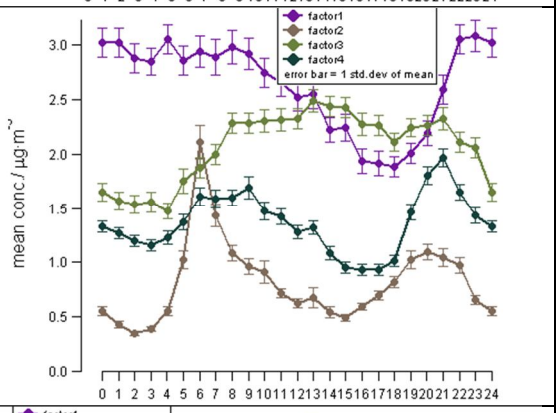
0.175	0.405	0.113	0.118	0.9078		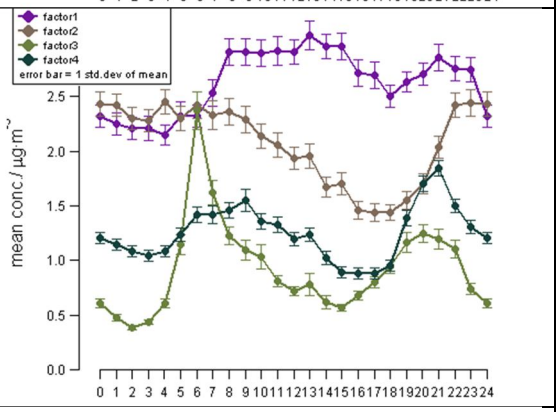
0.2	0.401	0.131	0.148	0.9530		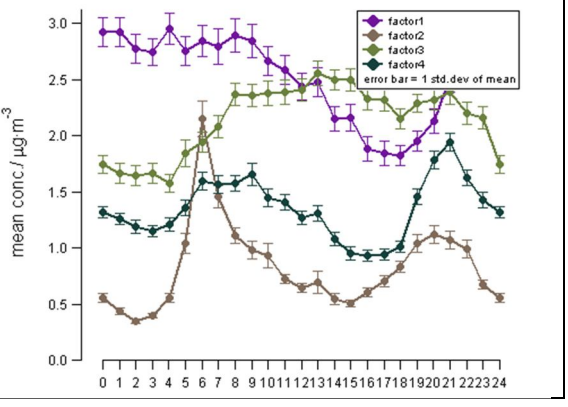

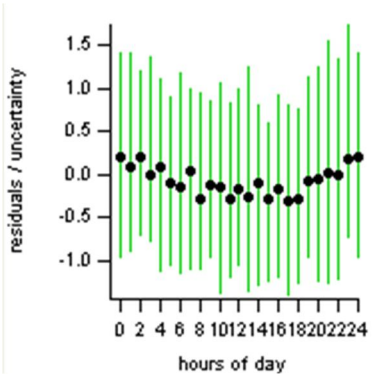

Figure S8. Residuals for m/z 55 for the 4 factors solution with constrained COA with a-value=0.1.

5 factors with constrained COA. It resulted in a split of the HOA factor, with the two resulting HOA factor contributions being correlated (R^2=0.533), while there was no correlation with the rest of the factors (R^2<0.06).

6 factors with constrained COA. A 6 factors solution was tested constraining a COA factor. The factor profile used as anchor profile was the COA profile that resulted from the 4 factors solution. It resulted in a split of the HOA factor, and a split of the SV-OOA factor, with the two resulting SV-OOA factor contributions being correlated (R^2=0.50).

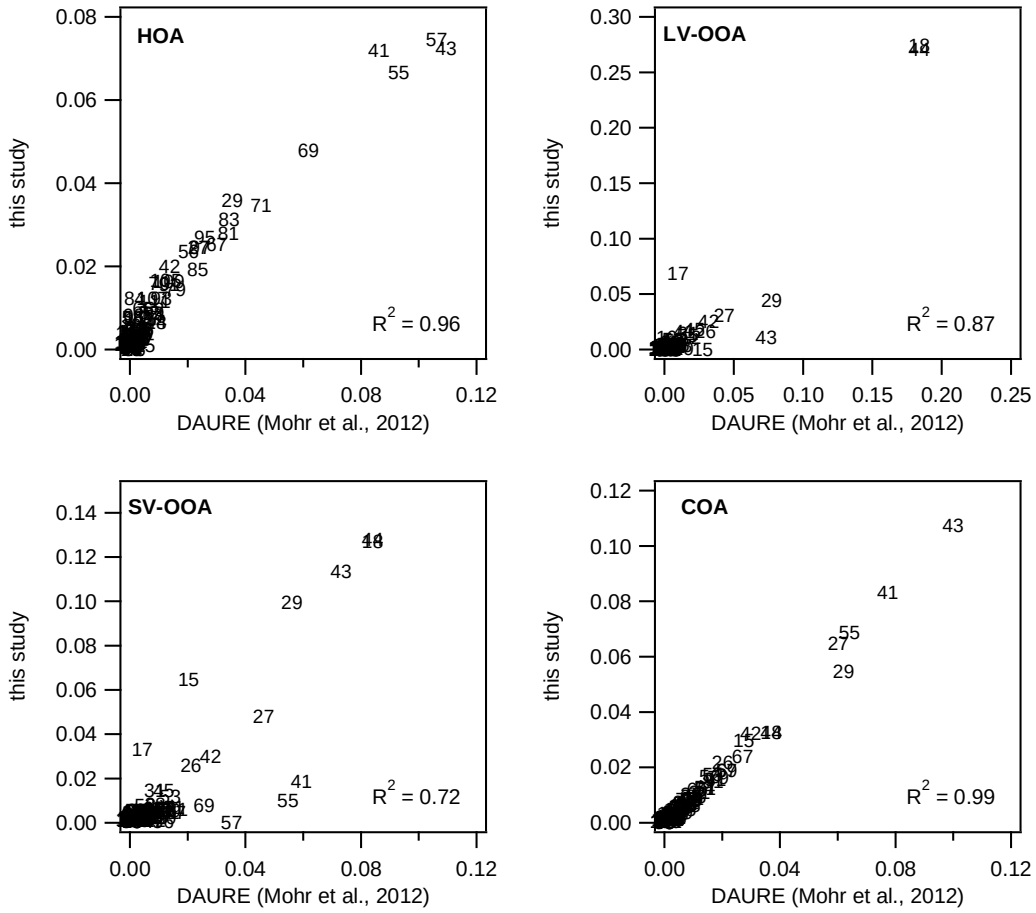

Figure S9. Mass spectral profiles from the OA sources/types identified in the present study compared with those found in Barcelona in the DAURE campaign in March 2009 (Mohr et al., 2012). Numbers correspond to the different *m/z*. Note that the COA is included for reference, but the high correlation is due to the use of the COA factor profile from DAURE as the anchor profile for the solution in the present study.

SECTION S4. ACSM details

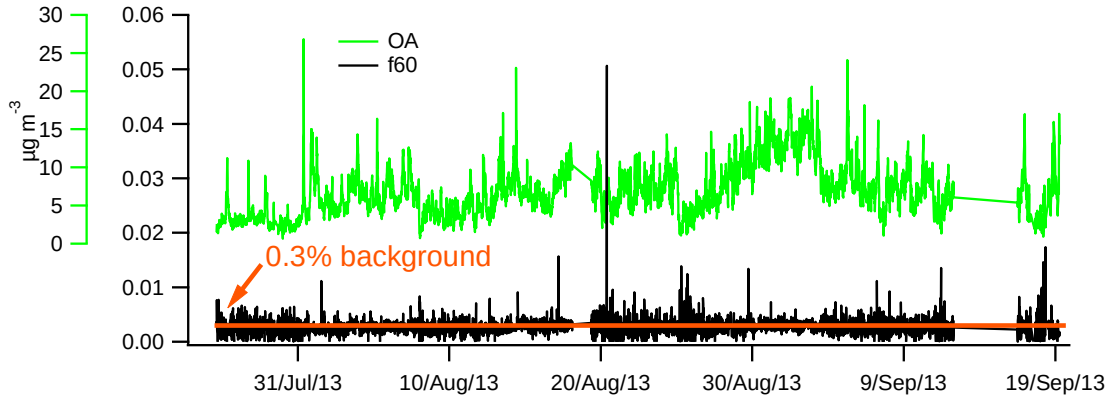

Figure S10. Time series of f60 (unitless) and OA concentration (µg m^{-3}). Orange line corresponds to the 0.3% background threshold for the f60 identified by Cubison et al. (2011).

SECTION S5. HOA/BC ratio variation

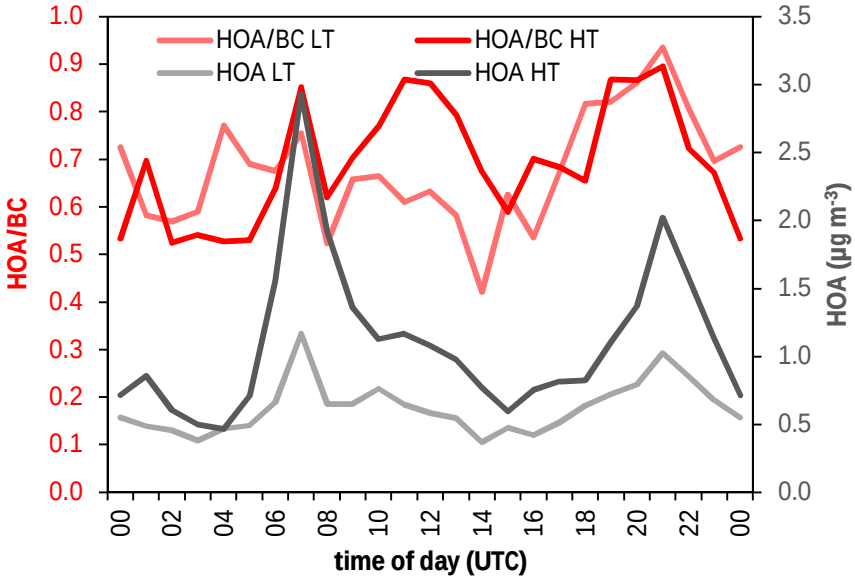

Figure S11. Average daily pattern of HOA and HOA/BC for the low traffic (LT) and high traffic (HT) periods.

SECTION S6. ^{14}C related information

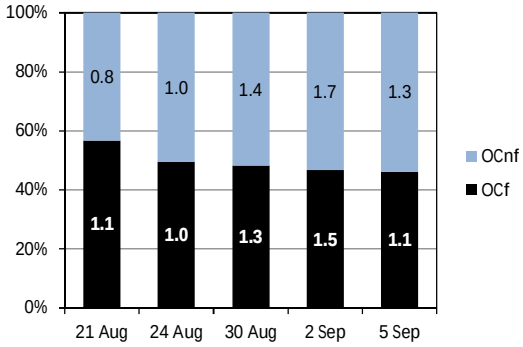

Figure S12. Proportion of non-fossil OC (OCnf) and fossil OC (OCf) in total OC from the selected samples.

REFERENCES

Budisulistiorini, S.H., Canagaratna, M.R., Croteau, P.L., Marth, W.J., Baumann, K., Edgerton, E.S., Shaw, S.L., Knipping, E.M., Worsnop, D.R., Jayne, J.T., Gold, A., Surratt, J.D., 2013. Real-time continuous characterization of secondary organic aerosol derived from isoprene epoxydiols in downtown Atlanta, Georgia, using the aerodyne aerosol chemical speciation monitor. Environmental Science and Technology 47, 5686-5694.

Cubison, M.J., Ortega, A.M., Hayes, P.L., Farmer, D.K., Day, D., Lechner, M.J., Brune, W.H., Apel, E., Diskin, G.S., Fisher, J.A., Fuelberg, H.E., Hecobian, A., Knapp, D.J., Mikoviny, T., Riemer, D., Sachse, G.W., Sessions, W., Weber, R.J., Weinheimer, A.J., Wisthaler, A., Jimenez, J.L., 2011. Effects of aging on organic aerosol from open biomass burning smoke in aircraft and laboratory studies. Atmospheric Chemistry and Physics 11, 12049-12064.

Draxler, R.R., Rolph, G.D., 2015. HYSPLIT (HYbrid Single-Particle Lagrangian Integrated Trajectory) Model access via NOAA ARL READY Website (http://ready.arl.noaa.gov/HYSPLIT.php). NOAA Air Resources Laboratory, Silver Spring, MD.

Mohr, C., DeCarlo, P.F., Heringa, M.F., Chirico, R., Slowik, J.G., Richter, R., Reche, C., Alastuey, A., Querol, X., Seco, R., Peñuelas, J., Jiménez, J.L., Crippa, M., Zimmermann, R., Baltensperger, U., Prévôt, A.S.H., 2012. Identification and quantification of organic aerosol from cooking and other sources in Barcelona using aerosol mass spectrometer data. Atmospheric Chemistry and Physics 12, 1649-1665.